Evaluating remote auroral kilometric radiation observations as a classification and predictive tool for substorms

james.waters@lam.fr

Waters, J. E., Lamy, L., Coxon, J. C.

Auroral Kilometric Radiation (AKR) and Substorms

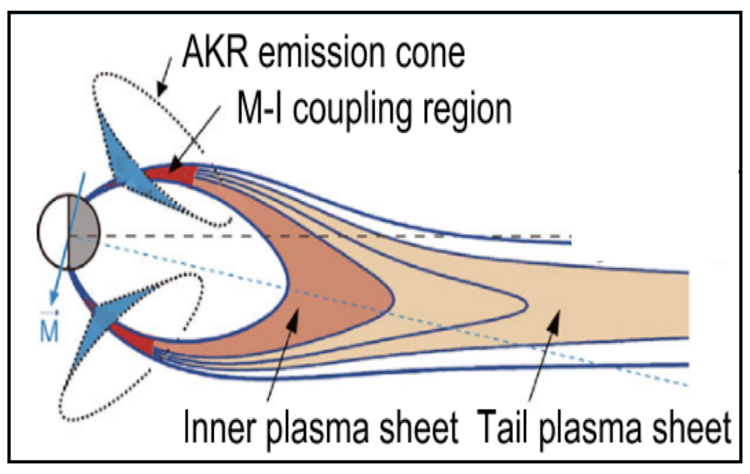

Figure 1: Schematic in meridional plane of AKR source region in context of magnetotail and MI coupling region, showing directed beaming cones from source in each hemisphere.

- **AKR** is radio emission **generated** on high-latitude magnetic field lines, **in the auroral acceleration region**, which **map to discrete auroral features.**
- The emission is **highly anistropically beamed**, so observations are highly dependant on observing position
- Increases in **AKR intensity indicates energetic electron acceleration**, while the **emission frequency** is linked to the **altitude of the active source region**.
- **AKR sources** show an **increase in radiated power at substorm onset**, with low frequency, **high altitude sources developing** (*Waters et al. 2022), i*n some cases **in the region of the Westward travelling surge** (*Waters et al. 2023*).
- **Substorms are dynamic processes** with a **broad range of observational proxies** in the magnetosphere, including geomagnetic indices such as SuperMAG SME/U/L (*Gjerloev 2012*), which have been **used to produce lists of events** that represent different dynamics in the timeline of substorm onset.
- We aim to **examine how 30 years** of **automatically selected AKR observations** with the Wind spacecraft could be used to **enhance current proxies or as a predictive tool,** by evaluating the **concurrence of substorm onset and AKR observations** while accounting for viewing.

Binary Classification

- **Existing metrics of substorm activity** (eg auroral morpholoy, magnetometer observations) can be used to **determine the forecastability of AKR observations.**
- Compute a **contingency table** where **defined time periods** are **examined for the concurrence of events** (see fig 2, true positives and true negatives in green, false positives and false negatives in red).
- Derived **classification statistics** can tell us how well **AKR observations characterise substorms** with respect to a given list.
- **Two event lists** from *Newell and Gjerloev* (*2011*) (NG11) and SOPHIE (*Forsyth et al 2015*), both **using SuperMAG**, are **used to define the presence of substorms** in time periods with fixed lengths or defined by the event list.
- We use **10 years** (1995-2004) of **AKR burst data** observed by Wind (*Fogg, Waters et al 2022*), and **consider observations from 6-hour-wide local time (LT) sectors centred on noon, dusk, dawn and midnight** (see fig 3).

Wind AKR bursts

Substorm List (SuperMAG)	Predicted positive	Predicted negative
Real positive	4599	8958
Real negative	5566	24701

Figure 2: Contingency table from fixed 2 hour blocks counting substorm onset events from Newell & Gjerloev (2011) SuperMAG based list, and Wind AKR bursts.

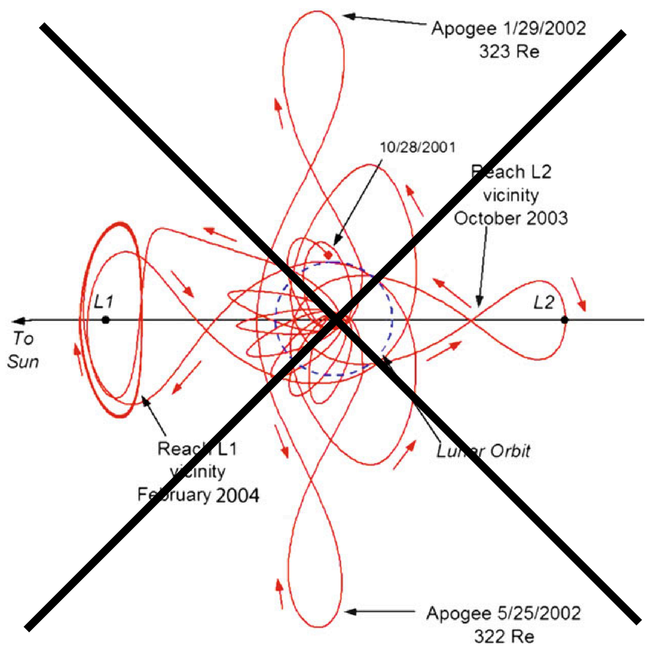

Figure 3: Illustration of the orbital trajectory of Wind between 2000-2004, before reaching L1, with LT sectors used in this work indicated.

With SuperMAG-based Event List from NG11

- For the **NG11 event list**, based on continuous SML decreases below fixed thresholds, **regular 2 hour blocks** covering the 10 year period **are counted as events** if they **contain one or more substorms** (see figure 4).

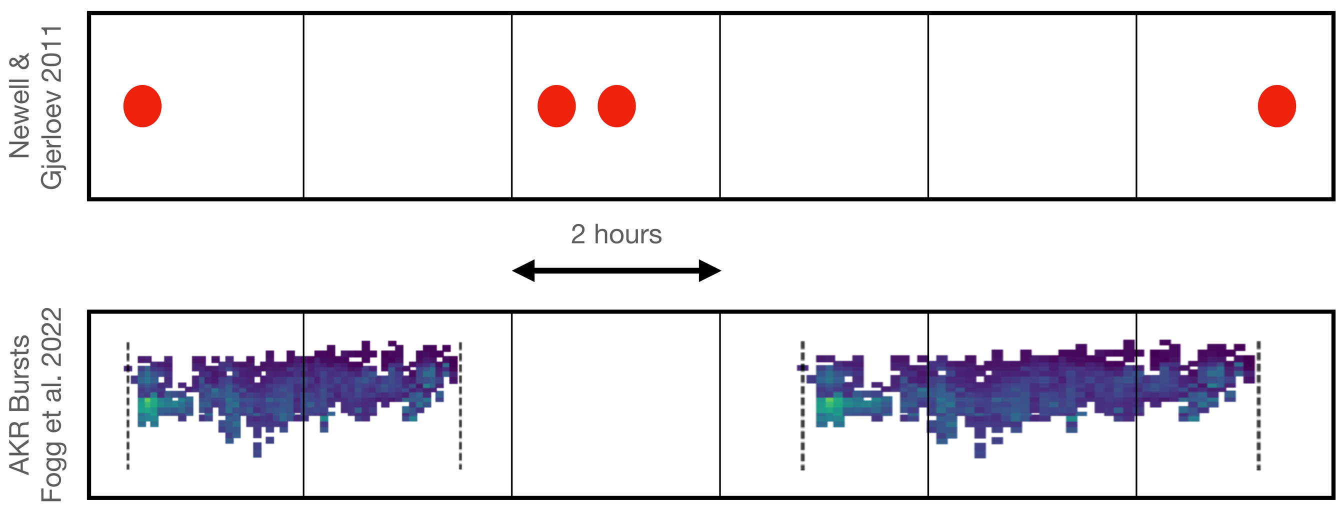

Figure 4: Schematic illustrating the event counting for the NW11 substorm list based on SuperMAG SML index. Red dots in the top row indicate the presence of a substorm onset in their list. Example AKR bursts are shown in the bottom row

- AKR bursts are counted, and **blocks are subset by the mean spacecraft LT**
- Figure 5a shows the **classification statistics**:
  - **Night- and dusk-side** observations have the **highest event recall**.
  - A **high false alarm probability** is also seen on the **nightside**, due to **prevalence** of **non-substorm-associated electron precipitation**.
  - **Dayside** observations have a **high miss rate**, but **low false alarm probability**.
- Figure 5b shows the **Heidke Skill Scores (HSS)**; **negative or zero values** indicate **poor predictive skill**, while **positive values indicate good skill**, with HSS = 1 indicating a perfect forecast.
  - **All LT sectors** have **positive predictive skill except the nightside**, likely due to the ubiquitous presence of non-substorm associated acceleration processes

Figure 5: (a, left) Classification statistics of AKR bursts observed in the 4 LT sectors, and all data combined. (b, right) HSS for each LT sector and all data.

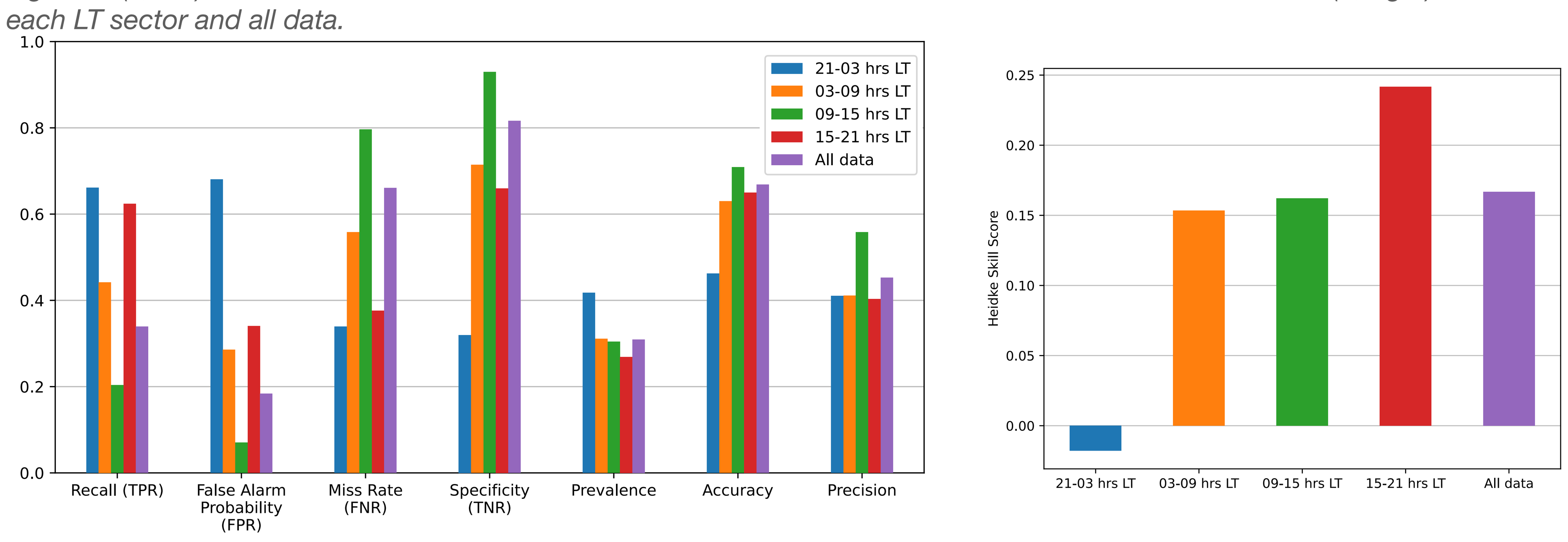

With SuperMAG-based Event List from SOPHIE Algorithm

- For the **SOPHIE event list** (*Forsyth et al. 2015*), a free statistical parameter (% EPT) allows **times of substorm expansion and recovery phases** to be **derived** based on the magnitude of the SML rate of change. **AKR has greater intensity** response on average **for substorms with a higher EPT**, which **begins up to 20 mins before onset** (*Waters et al, 2022*)
- SOPHIE 75% and 90% EPT lists are used, and **blocks are derived from expansion and recovery phases** (see figure 6).

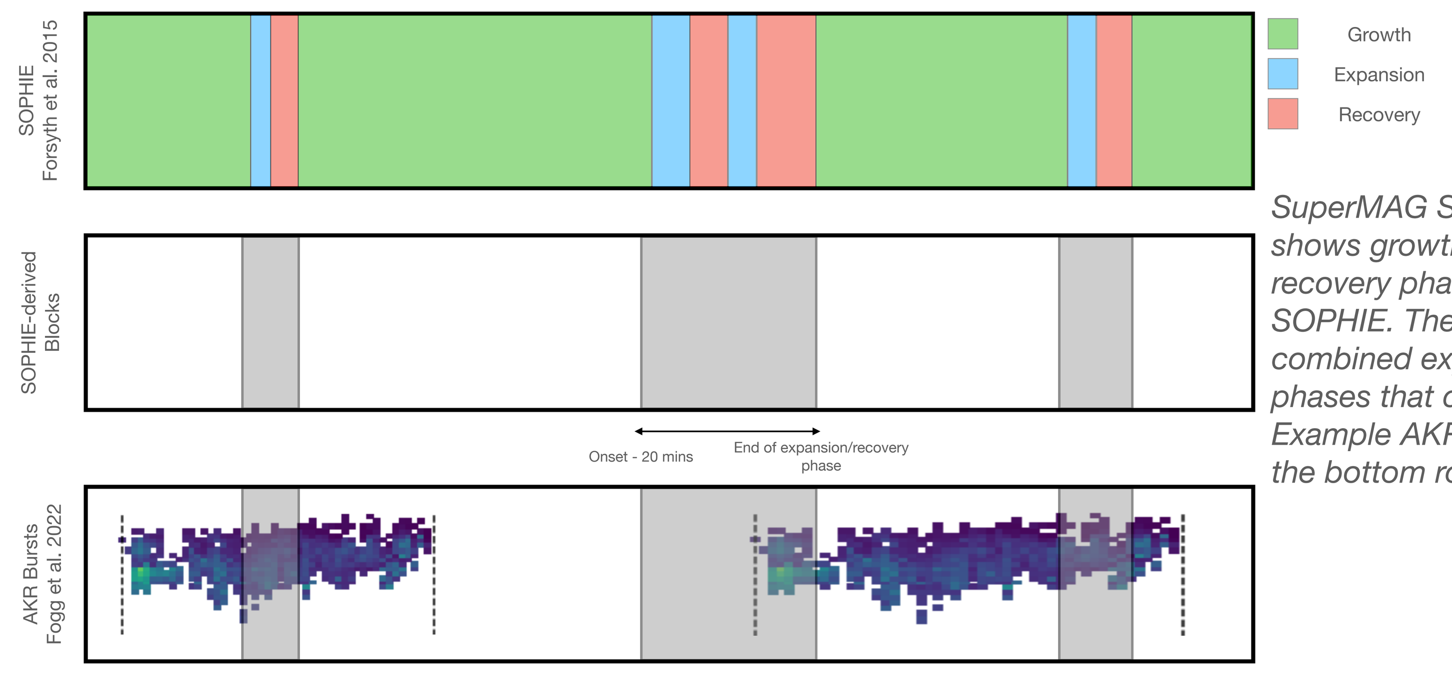

Figure 6: Schematic illustrating the event counting for the SOPHIE algorithm, based on the SuperMAG SML index. The top row shows growth, expansion and recovery phases output from SOPHIE. The middle row shows the combined expansion and recovery phases that define event blocks. Example AKR bursts are shown in the bottom row

- An **offset is subtracted from** expansion phase **onset**, with **analysis repeated** for offsets of **20-180 mins**.
- Figure 7 shows the **HSS for each LT sector** for increasing offsets; HSS of **most** LT sectors **correlate with the offset magnitude** (block durations also increase by default).
- **Positive HSS** result from the **75% list for all offsets**, while the **90% list** results in **positive HSS** for **timeshifts > 80 mins.**

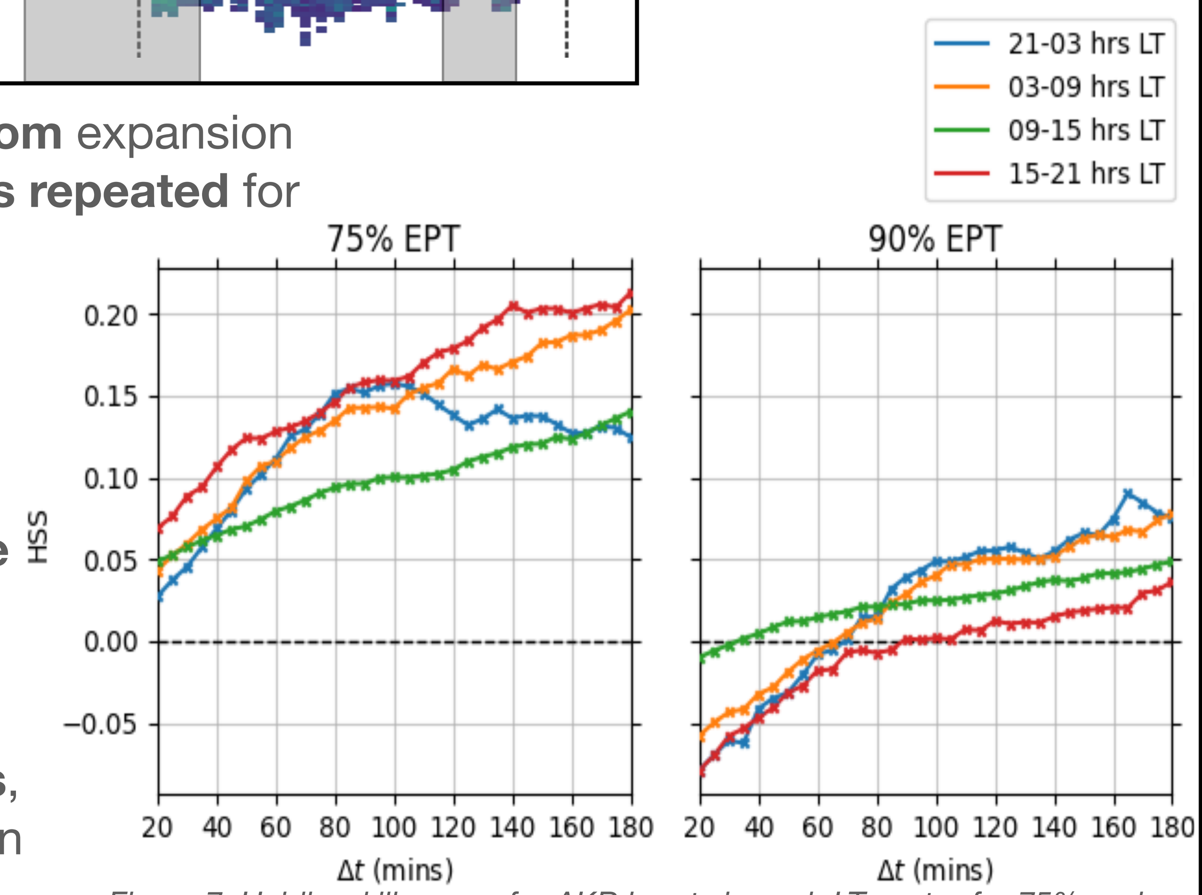

Figure 7: Heidke skill scores for AKR bursts in each LT sector for 75% and 90% EPT lists from SOPHIE, with increasing timeshifts Δt *subtracted from initial onset times.*

AKR Burst Frequency Distributions

- Comparing **occurrence of AKR burst frequencies observed** during blocks **with or without substorms** could help determine **whether future observations** are **substorm-associated**.
- Figure 8 shows the **distributions for the dusk- and day-side sectors**, for the NW11 list.
- **Except the dayside**, all LT sectors show a **lower median frequency for substorms**, indicating **AKR sources** at **higher altitudes** in the **acceleration region.**

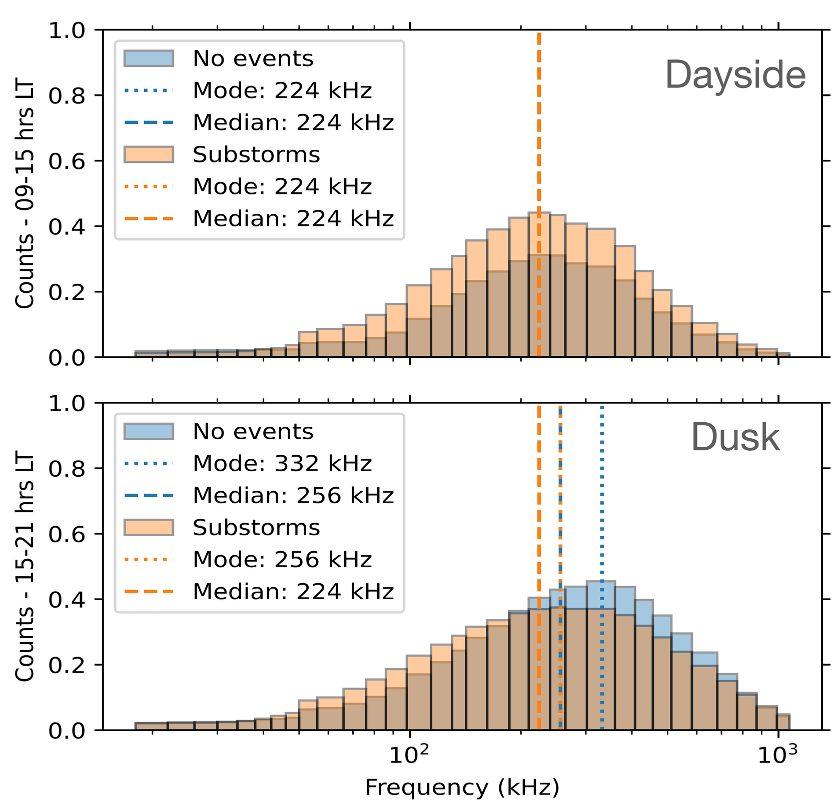

Summary and Future

- **AKR burst observations** have a **positive predictive skill** when comparing to substorm event lists based on the SuperMAG network **for most LTs**.
- **AKR observed from the nightside** has a **negative predictive skill** for the **NW11 list**, likely due to **ubiquity of acceleration processes. Duskside observations best characterise substorm activity** based on NW11 and SOPHIE 75% EPT lists.
- **Dayside observations** have a **high miss rate**, but a **low false alarm probability**, indicating **usefulness of L1 measurements**
- Examining **classification statistics** from substorm lists based on **other magnetospheric proxies** could highlight **most related phenomena** or event time
- Determining similar classification ability for other magnetospheric dynamics can explore fundamental differences in AKR characteristics (frequency, source LT).
- **Modelling visibility of AKR sources** with **beaming constraints** and **typical spatial distributions of substorms** will give **probabilistic perspective**.

cnes

LAM LABORATOIRE D'ASTROPHYSIQUE DE MARSEILLE

References

- Waters et al. 2022 [A]
- Waters et al. 2023 [B]
- Newell & Gjerloev 2011
- Gjerloev et al. 2012
- Morioka et al. 2013
- Forsyth et al. 2015

A

B